applied sciences

MDPI

Article

Numerical Assessment and Repair Method of Runway Pavement Damage Due to CBU Penetration and Blast Loading

Jaeduk Han, Sungil Kim and Injae Hwang *

Department of Protection and Safety Engineering, Seoul National University of Science and Technology, Seoul 01811, Korea; jaeduk@seoultech.ac.kr (J.H.); sung1.kim@seoultech.ac.kr (S.K.)
* Correspondence: injae2239@seoultech.ac.kr

Abstract: This paper addresses the protection capability of a runway pavement by executing a field blast test on an airfield pavement subjected to blast loading from a CBU (cluster bomb unit), and by confirming the numerical simulation of warhead penetration and the form of damage. The CBU's blast loading applies the BAP 100 of an air-to-ground munition in a similar scale. Penetration depth is calculated by a formula which incorporates the terminal speed of a free-falling cluster munition dispersed 20 km above the ground. According to the result of the calculation, the penetration depth by a cluster munition is 33 cm from the surface of the pavement. The field blast test was conducted based on this result. Furthermore, LS-DYNA software simulation was used to assess the condition of damage, determined by the depth of penetration and explosive pressure from a free-falling CBU landing on the airfield pavement from 20 km above the ground. The condition was ultimately used to verify the result of field testing and to confirm the scale of damage repair. The depth of explosion was 78 cm, from the surface to the crushed stone and sand layer below the pavement, and the diameter was 30 cm. The size of the crushed concrete that needed to be removed was an average diameter of 156 cm. The simulation result confirms that the diameter and depth of the crater are 67.6 cm and 67 cm, respectively, when the CBU is detonated under the same depth as the field testing, and the height of upheaval is 12 cm. The most appropriate method for repair, after a series of reviews, is to cut and remove a concrete slab 1.8 m × 1.8 m and cast the crushed stone layer disrupted from the explosion, followed by repairing the removed damaged concrete slab sections using rapid hardening concrete.

Keywords: airfield; pavement; concrete; blast; explosive; cluster bomb unit; runway repair; numerical assessment; M&S

Citation: Han, J.; Kim, S.; Hwang, I. Numerical Assessment and Repair Method of Runway Pavement Damage Due to CBU Penetration and Blast Loading. *Appl. Sci.* **2022**, *12*, 2888. https://doi.org/10.3390/app12062888

Academic Editor: Jungwhee Lee

Received: 23 December 2021
Accepted: 9 March 2022
Published: 11 March 2022

1. Introduction

The recent history of war verifies the importance of air operations in modern warfare, in which the outcome of a war is determined by the establishment of air superiority in the early phase of war. Therefore, neutralizing the enemy's capability to conduct air operations is a required condition for victory. In order to accomplish this objective, friendly forces need to attack enemy airfields first to restrain their air operations. The primary way to attack is changing these days: delivering cluster munitions with a TBM (Theater Ballistic Missile) or an AGM (Air-to-Ground Missile) to create multiple craters on the airfield is the preferred method [1]. On the other hand, some studies suggest that the asphalt concrete surface of the multi-layer pavement system can be used to absorb the dynamic energy [2]. However, flexible pavement is not suitable for airfields that normally operate jet aircraft, such as fighter jets, due to its vulnerability to heat. For this reason, most airfields use rigid concrete pavements. This study assesses the protection capability of the rigid concrete pavement from such attack by confirming the scale of damage from detonating explosives in field with the equivalent level of explosion of a CBU; and verifies the depth of penetration by a warhead and its damage condition, using LS-DYNA software. The objective of this

study is to verify the depth of penetration and the damage condition by modeling. For the modeling, a formula was used to compute the relationship between the height at which a warhead of CBU disperses and the depth of penetration into concrete pavement. A concrete pavement similar to that of an airfield was used for an actual explosive test on a live site in order to discover the scale and form of a crater. A cluster bomb unit delivered by a ballistic missile is normally dispersed approximately 20 km above the ground, then flies vertically before free falling onto the target. The speed of free fall allows a warhead to penetrate into the pavement surface followed by an explosion creating a crater. The study simulated by detonating the equivalent amount of TNT installed under the airfield pavement at the same level of depth, and ultimately confirmed the damage condition to the pavement. The field test applied the calculated result which assumes the depth with no penetration into the pavement. The test also confirmed that an explosion inside the concrete pavement creates a disruption due to its pressure, from the surface of pavement down to 78 cm deep where a sand layer is located; and the concrete slab deforms to approximately 156 cm due to upheaval, breaking, and other factors, consequentially limiting the overall traffic of aircraft and requiring removal of these objects. For the modeling results, the scale of damage was 67.6 cm in diameter and 67 cm in depth when running a model in the field test. When comparing the field blast test result and the result of numerical simulation, the latter ended up with a longer diameter and, thus, more severe damage. Additional analysis confirmed that the speed of explosion for the explosives used in the field test was 6000 m/s, which is slower than the speed of explosion for a genuine warhead at 7650 m/s. This was due to the shape of the tube. Since a genuine outer shell used for an explosive was not available, a cylindrical shaped tube was used instead to install the TNT. The shape of the tube, which was not in the spherical shape, ended up concentrating the explosion to the upper part of the pavement. Such penetration and explosive pressure of a CBU created a small crater. After some review, the appropriate way to repair the pavement was found to be removing the 1.8 m $\times$ 1.8 m concrete pavement sections where plastic deformation occurred and applying a high-early-strength concrete method [3,4].

2. The Depth of CBU Penetration

There are several formulas which can be applied to assess penetration depth into a concrete pavement. The US Army recommends assessing the depth of damage on a concrete panel in accordance with UFC 3-340-01 [5,6]. In order to assess the penetration depth into concrete, in order to design protection structures against impact loading, CONWEP, Army Corps, Haldar, Ammann and Whitney, UKAEA, BRL, Modified Petry, and Modified NDRC formulas can be used [7]. Therefore, this thesis used some of these formulas to assess the depth of penetration, and the result in which a pavement is not penetrated at all was selected to be used as the penetration depth at the field blast test.

2.1. Calculation of Penetration Depth

Even though the concrete's compressive strength is relatively stronger than its tensile strength, its tensile strength is approximately 1/10 of its compressive strength, which necessitates the use of rebar to minimize the tensile fracture or destruction from missile impacts. However, runway pavements are constructed with unsupported concrete without any rebar, and to reinforce its weak tensile strength, much stronger flexural strength is applied to its construction. CBU penetration depth onto concrete is experimentally found to be inversely proportional to the concrete's compressive strength $(f_c)^{0.5}$, and as the aggregate size increases, penetration depth decreases [8]. CBU penetration depth can be represented as a function of a missile's impact speed, its angle of impact, the mass of the projectile, and the shape of the projectile. United States Army and Ballistics Research Laboratory conducted numerous impact experiments on concrete and developed the CONWEP equation from the collected data. In 1946, the National Defense Research Committee (NDRC) conducted additional experiments based on above mentioned equation and developed an NDRC formula. This formula was made with quantitative measurement of impact response and

concrete penetration ability, based on a projectile's shape, such as warhead shape factor, missile shape, density, and speed. The revised NDRC equation, shown as Equation (1) below, includes the relationship between concrete's compressive strength and penetrability which they obtained from additional experiments [7]. Among many empirical formulas, this research used the NDRC formula in Equation (1) with the CBU warhead specification in Table 1 to calculate the penetration depth, with the assumption that the intrusion was 33 cm into the pavement surface.

$$G = \frac{180NW}{d\sqrt{f_c}}\left(\frac{v}{1000d}\right)^{1.8}, \ \frac{x}{d} = G + 0.9395 \ for \ G \geq 1.0605 \quad (1)$$

where

x = Penetration depth;
N = Nose shape factor;
W = Projectile weight;
d = Projectile diameter;
f_c = Compressive strength of concrete; v = Velocity of projectile.

Table 1. Cluster bomb and concrete pavement coefficient.

Projectile weight (W)	32 kg	Effective sectional area of projectile (A)	7.854×10^{-3} m^2
Projectile diameter (d)	0.1 m	Gravitational acceleration (g)	9.8 m/s
Shape coefficient (D)	0.3	Density of air (ρ)	1.2 kg/m^3
Velocity of projectile (v)	470 m/s	Compressive strength of concrete (f_c)	35 MPa

2.2. Field Trial Blast Test Result

If the explosive intrudes into the concrete and detonates, the explosive gives off strong pressure, gas, and high temperature heat. This pressure and heat melt or degrade concrete, and the explosion pressure fractures the pavement via shockwaves [9]. Therefore, the stress buildup inside the concrete exists as a shear stress centered around the point of explosion and forms rings of fractures at the fracture zone [10]. In Hwang's [11] live explosion experiment, a model runway was made to test an industrial explosive mimicking the CBU. The model airfield pavement was made up of 38 cm of concrete slab, 15 cm of stabilizing cement layer, 15 cm of crushed stone layer (drainage layer), and 15 cm of sand (separation layer). With the revised NDRC formula, the warhead intrusion depth was 33 cm for the following [12]. An industrial explosive (TNT) designed to replace the CBU was made by placing 4 kg of TNT, which has similar explosive strength to a CBU, in the perforated concrete structure. In this experiment on the runway pavement, the concrete layer was completely penetrated, and the sand layer was affected by the explosion due to its pressure and high temperature. This explosion pressure created a small explosion crater of 30 cm diameter and 78 cm depth from the surface of the concrete layer; it also created a fracture zone with diameter of 155.8 cm [11]. All of the runway pavement damage from the explosion is listed on Table 2. The explosion occurred with a 30 cm diameter circle. However, when the explosive was inserted into the perforated concrete instead of the outer warhead cover, the explosion was unable to impose spherical pressure to the concrete head. Instead, it applied tubular pressure which focused its explosion on to only the top and bottom of the structure, resulting in a weaker explosion than an actual CBU [11].

2.3. Verification of Field Test Results

During the contact explosion, explosive weight creates a crater while destroying the concrete or stone structures. When contact explosion occurs on the concrete slab, the explosion orb and pressure apply flexural stress onto the slab, which simultaneously destroys the back of the slab to create a hole [13]. However, since runway pavement is constructed on top of the foundation, the flexural stress has a lesser effect on the back of

the concrete slab. Therefore, when the warhead collides with the pavement surface, the intrusion and the explosive pressure penetrates from the face of the pavement, resulting in a crater. The radius of the crater from an impact explosion can be determined by the following Equation (2) below [14,15].

$$C = 18\,Kr^3 \Rightarrow r = \sqrt[3]{\frac{C}{18K}} \quad (2)$$

where

C = Weight of Explosive (kg);
K = Specific Charge Weight (kg/m^3);
r = Radius of Crater.

Values of specific charge weight, K, are represented in Table 3. If these values and the 4 kg TNT used in the field test were applied to Equation (3), crater radius can be calculated as follows.

$$r = \sqrt[3]{\frac{C}{18K}} = \sqrt[3]{\frac{4}{18 \times 3}} = 0.4\ \text{m} \quad (3)$$

Table 2. Result of the Damage and Repair Range.

Sort	Result of Field Test	Sort	Repair Range
Diameter	30 cm	Cutting and Removal Area	1.8 m × 1.8 m
Depth	78 cm	Repaired Depth	84 cm
Damage layer	Separation layer (Sand layer)	Repaired layer	Separation layer (Sand layer)
Upheaval	0~0.7 cm		
Fracture zone	155.8 cm		

Table 3. Values of Specific charge weight, K [14].

Material	K (kg/m^3)
Masonry	1.2–2.0
Plane Concrete (29 MPa)	2.5–3.0
Reinforced Concrete (without cutting reinforcement)	8.4
Reinforced Concrete (with partial cutting of reinforcement)	33.6

According to the calculation above, with compressive strength of the concrete is 29 MPa, the explosion crater has a radius of 0.4 m or diameter of 0.8 m. Furthermore, in 2012, research conducted by Hong Hao et al. [16] used programs such as LS-DYNA to conduct M&S (Modeling and Simulation) according to the weight of the explosives. These simulation results are shown in Figure 1 below.

In the LS-DYNA simulation result seen in Figure 1, concrete compressive strength of 41 MPa, 3.6 kg of explosives, and explosives intrusion of 0.75 m were used to simulate the crater diameter of 0.97 m [16]. When these simulation results were compared with the field test, the field test crater diameter was smaller by 0.3 m, while the depth was deeper into its sand layer. Since the field test explosives were installed 33 cm from the bottom of a drill-perforated concrete structure, the discrepancy between the field test and the simulation may be from the Munroe effect or Neumann effect. The Munroe effect or Neumann effect describe a phenomenon in which the explosives' energy gets concentrated onto a hole or a sliced surface during an explosion. This resulted in explosive pressure being concentrated on the top and bottom of the concrete structure, therefore, LS-DYNA simulation was altered to address this problem seen in the field test.

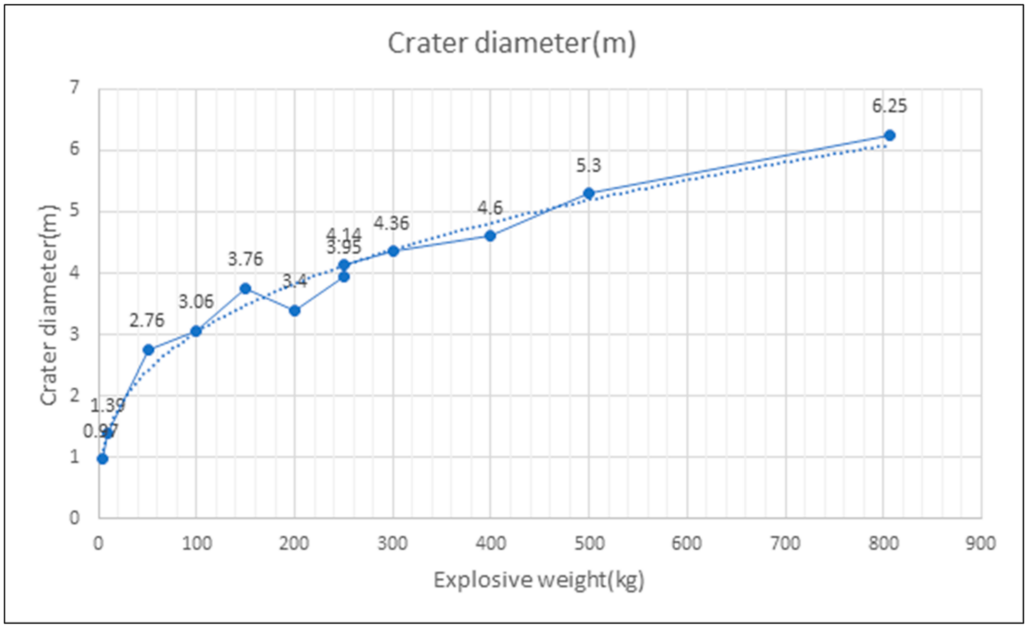

Figure 1. Crater Diameter by LS-DYNA M&S.

3. Numerical Simulation (LS-DYNA M&S)

Numerical modeling is a useful tool to check results similar to those of field tests for many structural problems that cannot be tested in the actual field. The modeling can reasonably predict economically desired results without conducting field testing or a test in a large lab, and it can sometimes replace other tests that are time-consuming and costly, such as the test to find out the structural process of loading from earthquake and blast loading [17]. Therefore, in this research, the numerical simulation using finite elements through LS-DYNA software was performed to compare and evaluate the field blast test results, and the protection capability against the pressure generated by the explosion of a warhead penetrating the pavement.

3.1. Construction of Simulated Runway Pavement

For the modeling of materials, it is necessary to combine and analyze the Lagrangian method and the Eulerian method; the former is for numerical analysis of solid materials in order to interpret the multi-layered airfield pavement system; the latter is for numerical analysis of explosive pressure [18]. The modeling of solid materials consists of concrete slabs, subbase, and continuum for bedrock, in order to model the multi-layered airfield pavement. The explosion in the current numerical model is symmetrical to the spherical explosion, meaning that a pressure pulse occurs. In order to reduce the time for analysis, the point of explosion, as shown in Figure 2, was chosen to be the center as well as a quarter of the entire model, in order to confirm the form of the explosion. The RHT Concrete Model was applied for the concrete materials, and the Mohr–Coulomb Model was applied for the materials used for a base course, such as crushed stone. In addition, the Simplified Johnson–Cook Model and the High Explosive Burn Model were applied to model the penetration of a warhead and the explosion, respectively. For the EOS of the explosion, Jones–Wilkins–Lee (JWL) was applied [19–21].

The field test is an experiment to confirm the scale of damage by TNT, which has the same weight level as the CBU warhead, penetrating 33 cm below the pavement in accordance with the formula, under the assumption that the freefalling cluster bomb unit does not penetrate the concrete pavement. The numerical simulation for modeling also installs and detonates the same size of PBXN-109 33 cm below the pavement. The 3D numerical model applied in this simulation only models a quarter of the concrete slab,

considering the symmetry. The material properties of the concrete slab are as follows in Table 4.

For the material properties of the explosive device, the Density (ρ) was 1680 kg/m^3, and the Speed of Explosion (v) was 7650 m/s, which is the average explosion speed of PBXN-109 [22].

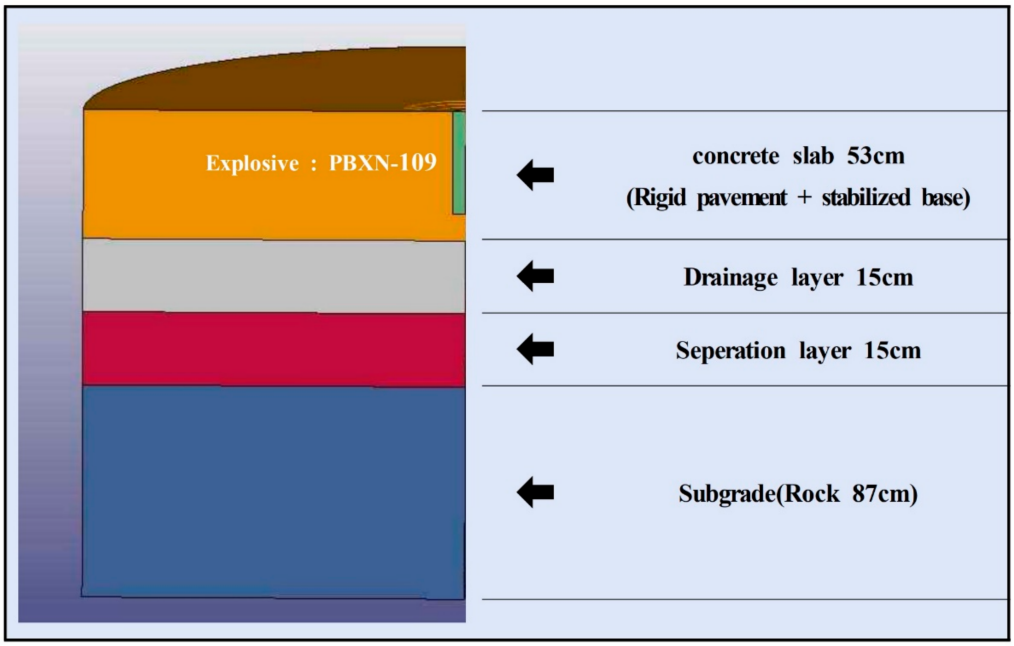

Figure 2. Field test M&S model.

Table 4. Material properties of concrete slab for the model.

Parameters	Symbol	Units	Value
Young's modulus	E	GPa	27
Compressive strength	f_c	MPa	3.5
Shear modulus		GPa	16.7
Density	ρ	kg/m^3	2314

3.2. RHT Concrete Model and Material

Concrete is a brittle material made up of cement paste, small aggregates, and large aggregates. The RHT (Riedel–Hiermaier–Thoma) model is a material model that was introduced in 2004 using ANSYS AUTODYN by Riedel, Hiermaier, and Thoma as a hydrocode that can well represent such brittle materials. After its development, this material model was added as one of the LS-DYNA material models. The RHT Concrete (RHTC) model is specific toward concrete among many brittle materials. It is a macro model that possesses the ability to well describe the dynamic strength of concrete in response to an impact or outside pressure [23]. Additionally, since it considers plastic behavior instead of elastic behavior, it can be used to model high speed impact distribution more accurately than other models. Even though you must input more than 30 parameters to use the RHTC model, Riedel's CONC-35 parameter set can be used for concrete with 35 MPa compressive strength.

The RHTC model is a model that combines shear and pressure. It uses Herrmann applied equation of state (EOS) to describe the hydrostatic behavior of concrete. Figure 3 represents the p-α equation of state graph for a porous material.

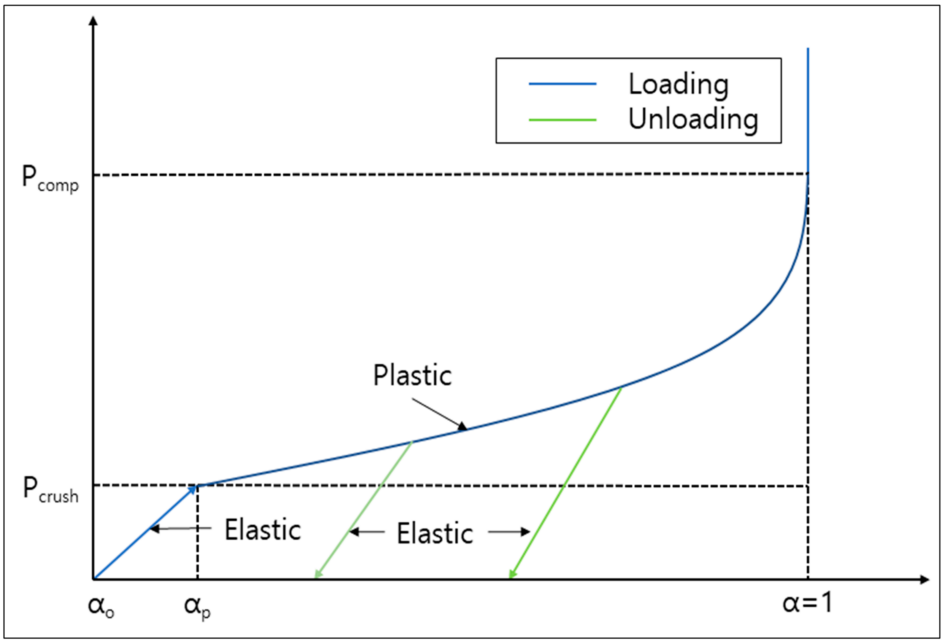

Figure 3. Schematic description of the p-αequation of state [Herrmann, W. et al., 1969].

In the RHTC model, the material that fills up the void space of the matrix is represented using the polynomial equation of state shown in Equation (4) below.

$$p = \begin{cases} A_1\mu + A_2\mu^2 + A_2\mu^3 + (B_0 + B_1\mu)\rho_0 e \; if \; \mu \geq 0 \\ T_1\mu + T_2\mu^2 + B_0\rho_0 e \; if \; \mu < 0 \end{cases} \quad (4)$$

where

p = Pressure;
A_1, A_2, A_3, B_0, B_1, T_1, T_2 = Constant;
e = Internal energy.

For the porous material calculation, there needs to be additional formula regarding the porosity of the material which follows the Herrmann formula shown in Equation (5). This formula is a pressure-dependent equation that was used in AUTODYN's RHTC model.

$$\alpha(p) = 1 + (\alpha_p - 1)\left(\frac{p_{comp} - p}{p_{comp} - p_{crush}}\right)^n \quad (5)$$

where

α = Porosity ratio;
p = compaction pressure;
p_{crush} = Pore crush pressure (Initial compaction pressure);
p_{comp} = Solid compaction pressure.

In LS-DYNA, porosity is represented by time depended Equation (6) below.

$$\alpha(t) = \max\left(1, \min\left(\alpha_0, \; min_{s \leq t}\left(1 + (\alpha_0 - 1)\left(\frac{p_{comp} - p(s)}{p_{comp} - p_{crush}}\right)^n\right)\right)\right) \quad (6)$$

The RHTC model represents fracture surface using yield strength, breaking strength, and residual strength. As the strain material increases past the breaking point of the material, the hardness, tensile strength, and resistance increase greatly, resulting in strain hardening. This strain hardening parameter was obtained using the researched concrete strain hardening information and applying it to a mathematical model. Yield strength is defined as a part of breaking strength with a cap, and this breaking strength is described by Equation (7).

$$Y_c(p^*) = f_c \times \left[A \times \left(p^* - {p_{spall}}^* \times F_{rate}(\dot{\varepsilon})\right)^n\right],\ {p_{spall}}^* = f_t/f_c \tag{7}$$

where

f_c = the material's uniaxial compressive strength;
f_t = the material's tensile strength;
p^* and ${p_{spall}}^*$ = pressure and spall strength, respectively;
$\dot{\varepsilon}$ = strain rate;
n = porosity exponent;
$F_{rate}(\dot{\varepsilon})$ = function of the DIF (Dynamic Increase Factor).

Equation (7) is related with Lode angle, θ, and decreasing strength during tri-axial tension can be represented by Equations (8) and (9) below.

$$R_3(\theta,\ p^*) = \frac{2\left(1-Q^2\right)\cos\theta + (2Q-1)\sqrt{4(1-Q^2)\cos^2\theta + 5Q^2 - 4Q}}{4(1-Q^2)\cos^2\theta + (1-2Q)^2} \tag{8}$$

$$Q = Q_0 + B{\cdot}p^* \tag{9}$$

where

$R_3(\theta,\ p^*)$ = function of Lode angle;
Q = Portion of the equivalent strength;
B = Reflects a brittle-to-ductile transition;

Q is a linear equation of normalized pressure, p^*, B is the fracture surface's transition number under increasing pressure, and residual strength is the exponential function of p. The RHTC model contains many constants and variables to describe compressive strength, tensile strength, shear strength, and other concrete behavior parameters. These constants and variables are determined by numerous and diverse experiments [24]. In this research, parameters inputted for modeling concrete pavement in the RHTC model are shown in Table 5.

Table 5. RHTC Model Material Information.

Material	**Density**	**Elastic Shear Modulus**	**Eroding Plastic Strain**	**B_0**
Concrete	2314 kg/m^3	16.70 GPa	0.5	1.22
B_1	T_1	A	N	Compressive strength
1.22	35.27 GPa	1.6	0.61	35 MPa
Relative shear strength	Relative tensile strength	Q_0	B	T_2
0.18	0.1	0.6805	0.01	0.0
Reference compressive strain rate	Reference tensile strain rate	Break compressive strain rate	Break tensile strain rate	Compressive strain rate dependence exponent
3.0×10^{-8}	3.0×10^{-9}	3.0×10^{-22}	3.0×10^{-22}	0.032
Tensile strain rate dependence exponent	Pressure influence on plastic flow in tension	Compressive yield surface parameter	Tensile yield surface parameter	Shear modulus reduction factor
0.036	0.001	0.53	0.7	0.5
D_1	D_2	Minimum damaged residual strain	A_f	N_f
0.04	1.0	0.01	1.6	0.61
Gruneisen Gamma	A1	A2	A3	Crush pressure
0.0	35.27 GPa	39.58 GPa	9.04 GPa	23.30 GPa
Compaction pressure	Porosity exponent	Initial porosity		
6.0 GPa	3.0	1.1884		

The values of 35 MPa for compressive strength, 2314 kg/m^3 as density, and 4.5 MPa for tensile strength were used to match airfield runway pavement strengths. In addition, for other parameters resulting in 35 MPa compressive strength, Riedel's CONC-35 parameter library was used [25].

3.3. Results and Analysis of Modeling

After drilling the concrete pavement surface, explosive PBXN-109 was installed at 33 cm below the pavement surface to simulate the explosion. As a result, as shown in Figure 4, the pavement surface suffered a 33.8 cm radius of damage from the center; the depth of damage including the upheaval was 67.2 cm; and the depth from the pavement surface was 55.2 cm.

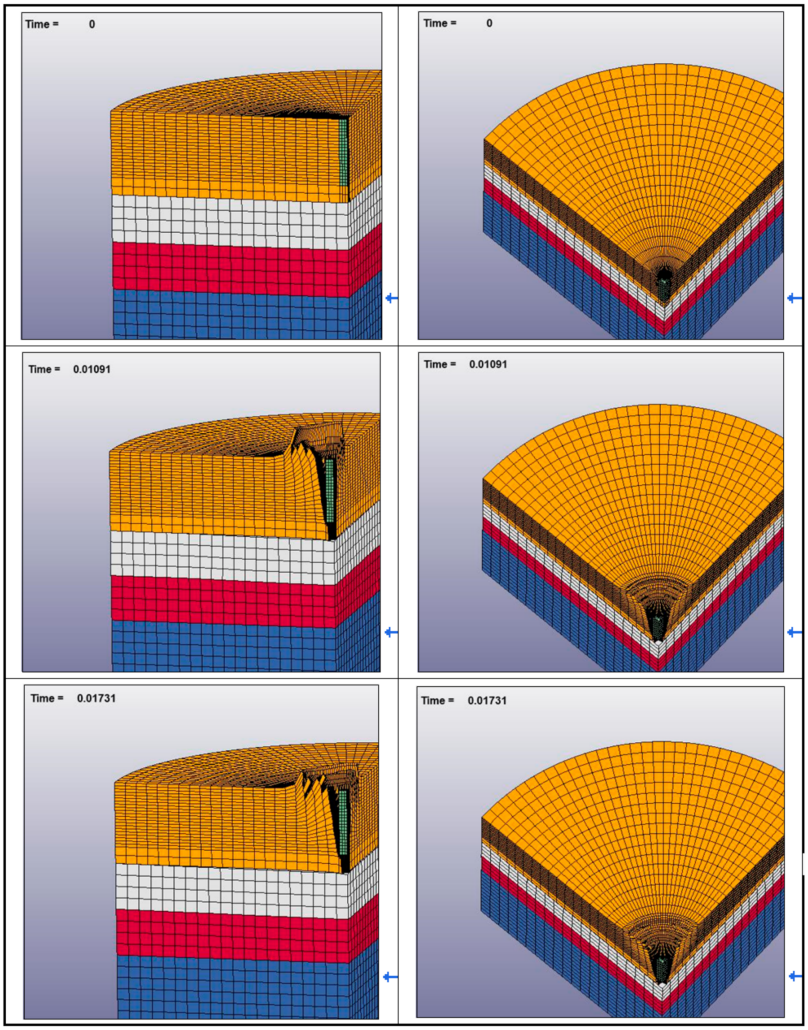

(**a**)

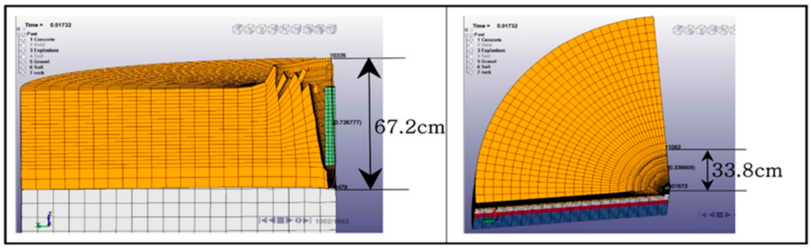

(**b**)

Figure 4. Result of the pavement damage: (**a**) Fracture shape by time; (**b**) Crater width and depth.

As shown in Figure 5, the strain rate and pressure distribution were simulated to cause deformation throughout the base course. Furthermore, the height of the upheaval on the concrete pavement surface, caused by the impact of the explosion, was measured to be about 12 cm from the existing surface. The damage to the crushed stone layer was very small at 2 cm, and this result was due to absorbing a significant portion of the blast pressure from the stabilizing base course because the cement stabilizing base course was applied at 15 cm.

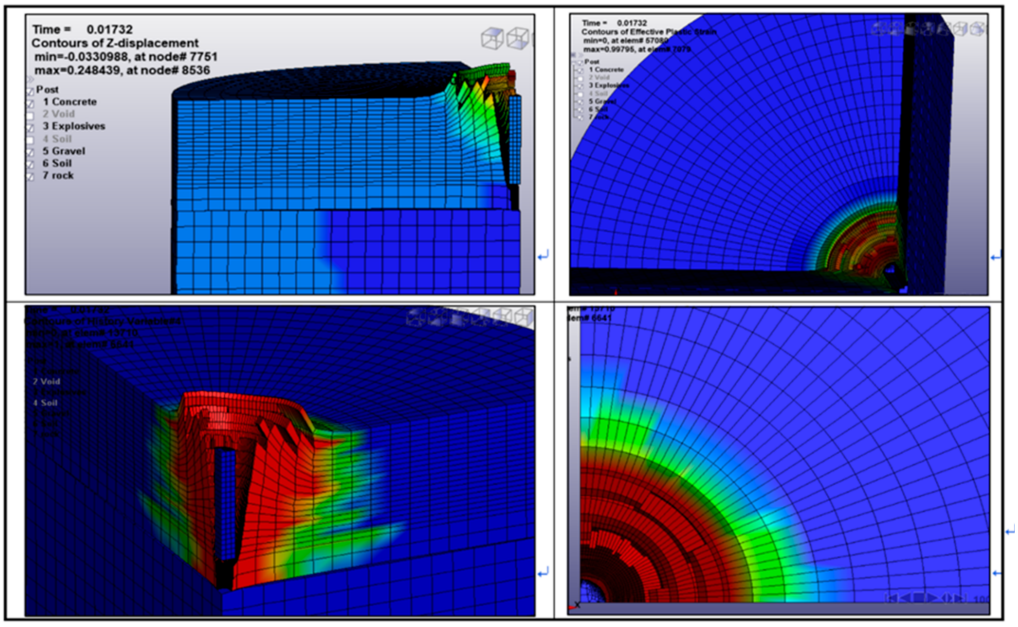

Figure 5. Result of strain and pressure.

Kinetic energy curve as a function of time is shown in Figure 6. In Figure 6, initial energy decreased rapidly after hitting 2.35 MJ. Additionally, Figure 7 shows that rapid displacement occurred during the explosion's initial burst of energy.

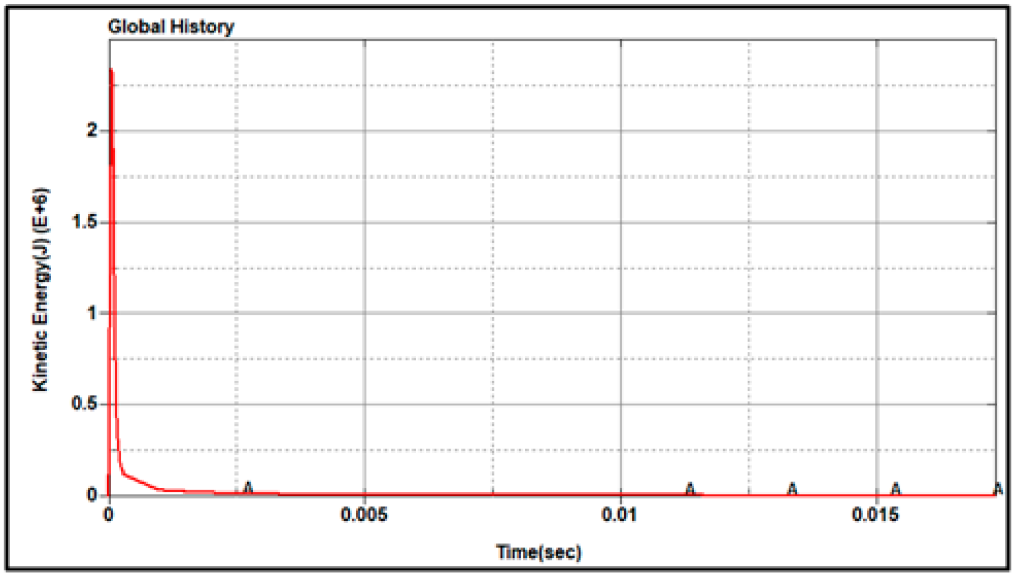

Figure 6. Kinetic Energy curve.

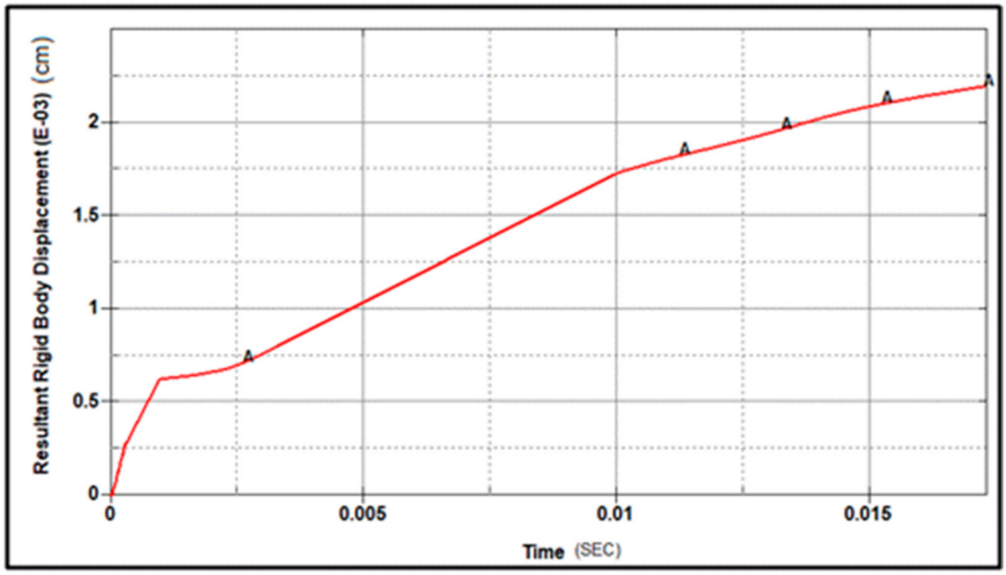

Figure 7. Displacement curve.

3.4. Comparison and Discussion with Regard to the Results of Numerical Simulation

At the field test, the damage on the concrete pavement was a small crater 30 cm in diameter and 78 cm in depth. In addition, as a result of the damage measurement conducted after the formation of the crater, cracks were generated along with 0–7 mm of upheaval on the concrete pavement due to the spread of the explosion pressure; a fracture zone was formed on the concrete slab up to an average diameter of 155.8 cm; and cracks were generated across the entire pavement. The numerical simulation result through the LS-DYNA program, under similar conditions, showed that the crater on the pavement surface had a diameter of 67.6 cm from the center; the depth of the damage was 67 cm including the upheaval on the pavement; and the displacement occurred throughout the base course. Furthermore, the height of the upheaval on the concrete pavement surface, caused by the impact of the explosion, was measured to be about 12 cm from the existing surface. The result of the computer simulation confirmed that a larger scale of damage occurred compared with the actual explosion test site, with a difference of around twice the diameter and 11 cm in the height of upheaval. The field test and M&S results are shown in Table 6.

Table 6. Comparison of the field test and M&S.

Sort	Field Test	M&S
Crater Diameter	30 cm	67.6 cm
Crater Depth	78 cm	55.2 cm
Damage layer	Separation Layer	Drainage Layer
Upheaval	0~0.7 cm	12 cm

The computer simulation results presenting different results from the explosion test site suggest important causes as follows. First, an industrial explosive called MegaMEX, which has a speed of explosion at 6000 m/s, was used at the field blast test. Compared with the explosion speed of the explosive PBXN-109, which was applied in the simulation, the MegaMEX had a slower speed of explosion during the explosion test. As a result, the power of the explosion was smaller than the reality. Next, the TNT was mounted in a cylindrical tube and installed at the concrete boring part, since the design of an actual outer shell for the explosive was limited. As the shape of the tube was cylindrical and not spherical, small damage occurred on the pavement, caused by the pressure induced to the upper part of the tube. Finally, the modeling incorporated a high compression level by applying properties

similar to the pavement surface, while for the field test the concrete properties of the cement stabilization layer was made with general concrete which has a low compression level. These causes and results confirm that it is necessary to utilize the field test results and numerical simulation results in a complementary manner. However, the recovery section is 1.8 m × 1.8 m in size and about 84 cm in depth, meaning that some parts of the crushed stone and sand layer need to be repaired. For this reason, the damage repair sections which encompass the concrete pavement and the plastic deformation sections can produce similar results [26].

4. Proposal of Crater Repair Method

4.1. Application of the Damage Repair Section

After the cluster bomb explosion, one must conduct leveling to check damage to the slab, and qualitative observation to check on the length, width, and the shape of the fracture. When the cluster bomb is intruded into the pavement and explodes, the high heat and pressure creates a crater and fractures. Ordinarily, to repair the crater, one must observe the cracks and fracture zone created by the explosion to determine where FOD (Foreign Object Damage) is possible and remove it. According to the damaged area representation by M&S, the region of deformation needing repair, including the ridges of the crater and the area of pavement plastic deformation, is 1.8 m wide, which includes the 155.8 cm fracture zone seen from the field test. The cracks or fractures from the warhead intrusion and explosion require reconstruction after removal for aircraft safety. For the convenience of this reconstruction, a 1.8 m × 1.8 m square region centered around the crater must be removed and the damaged drainage layer must be removed 0.7 m from the surface. Afterwards, the removed drainage layer must be refilled with gravel or other small aggregates before filling up the hole. An emergency pavement repair plan is shown in Figure 8. The repair for the cement stabilization layer should be done based on the field status if it was included in the original pavement.

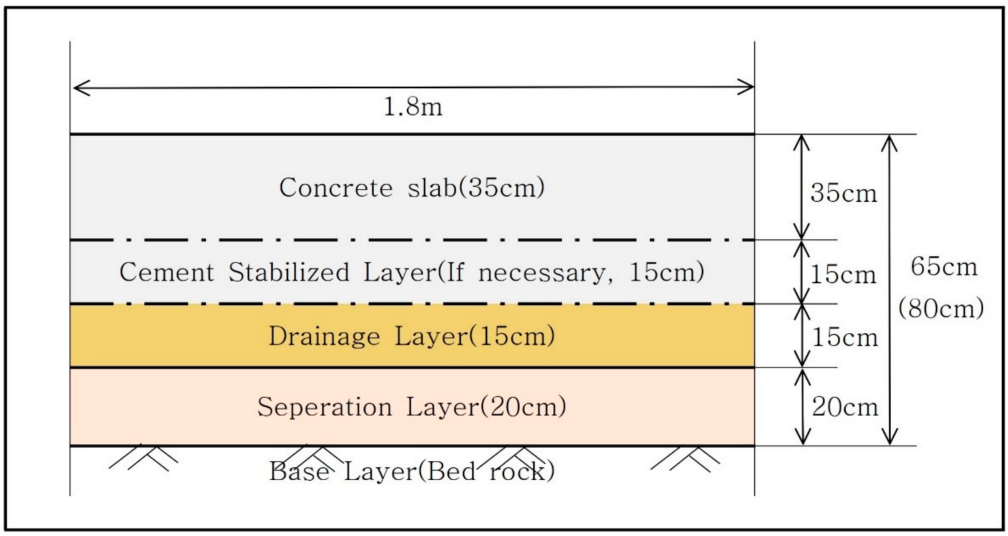

Figure 8. Runway rapid repair section.

4.2. Proposal of Rapid Damage Repair Method

Based on the field test and the M&S, Figure 8 shows the repair area of 1.8 m × 1.8 m and repair depth of 0.7 m including the drainage and separation layer. Therefore, the rapid repair method should be on a small crater scale. The use of FFM or AM-2 mat cover designed for 550 lbs (250 kg) explosive attack is insufficient for such damage. These mats are 18.3 m × 16.5 m (60 ft × 54 ft) which makes them too large compared to the crater. Furthermore, since CBU creates multiple craters, this method would require a longer repair time and an excess number of mats. Therefore, in order to propose a repair method suitable

for specific damage, the advantages and disadvantages of different methods are presented in Table 7. The emergency repair of the airfield runway must take time of war into account and must be done safely and efficiently. The emergency repair must be done quickly, efficiently, economically, and without any further repair.

Table 7. Comparison and assessment of small crater repair methods.

Repair Method	Advantages and Disadvantages	Applicability
High-Early-Strength Concrete	■ Able to simulate the concrete's strength early; ■ High durability after the repair; ■ Able to combine and construct based on the field's need; ■ Decent storage time for the construction material; ■ Expensive and has weather restrictions for the construction.	○
Precast Concrete (PCC)	■ High quality concrete same as the original pavement; ■ Able to craft precast panel and store it permanently; ■ Can be constructed regardless of the weather; ■ Expensive and must consider complex distribution; ■ Must remove more than the damaged part due to precast panel.	△
FOD Cover Mat	■ Easily applied; ■ Reusable; ■ Short-lived and incompatible with some airplanes; ■ Unsuitable for small craters and needs to be replaced.	×
Asphalt Concrete	■ Economic initial construction fee; ■ Usable for any shape crater due to its flexibility; ■ Sensitive to temperature change, therefore, incompatible with jets; ■ Different from original pavement and needs replacement; ■ Unusable for long term.	×

According to the advantages and disadvantages comparison in Table 7, there are two methods suitable for CBU pavement damage repair. The first method is HES (High-Early-Strength) concrete, which seems most suitable for emergency repair. This method uses on-site mixed cement and may be sensitive to temperature. However, this method allows the material to obtain the desired strength early, has high durability, and does not depend on the shape of the crater, making it most suitable for small crater emergency repair. The second method is the precast concrete method. If 1 m × 1 m or 2 m × 2 m sized panels can be prefabricated based on necessity, it may be used for some cases. The prefabricated panels are kept in storage until damage occurs, and this method requires the damaged area to be cut to match to panels. However, it can be used regardless of the weather conditions. Hence, after comparing different methods of emergency repair for CBU pavement damage, HES is introduced as the most suitable method. In addition, the precast concrete method is proposed as a method of replacing the HES method depending on the situation of the field.

5. Conclusions

This study confirmed the scale of damage to the airfield pavement from a CBU attack through a field test and verified the result through numerical modeling. In the event of a CBU attack by a ballistic missile, when the cluster munitions are dispersed 20 km above the ground, it penetrates the concrete pavement at the terminal speed of about 500 m/s by free fall, and the penetration depth was calculated to be 33–39 cm using the formula. Assuming that the CBU does not penetrate the pavement, an explosive was penetrated and detonated at 33 cm under the simulated runway for the field blast test, and the test confirmed that the crater was 300 mm in diameter; the fracture zone was 155.8 cm on average from the center of the crater; and the fracture zone had an upheaval and cracks for up to 0~7 mm

and 1~2 mm, respectively. The crater as a result of the modeling was 67.6 cm in diameter, and 67 cm in depth including the upheaval, and the displacement occurred throughout the base course. In addition, the height of the upheaval on the concrete pavement surface, caused by the impact of the explosion, was approximately 12 cm from the existing surface. Therefore, the model confirms that even some parts of the crushed stone and sand layer need repair, as the repair section is 1.8 m × 1.8 m in size and approximately 84 cm in depth. If damage occurs down to the crushed stone and sand layer, considerable time is additionally required for repair. It is necessary to change the construction standards to prevent penetration damage to the pavement, in the event of an explosion, by increasing the strength or thickness of concrete. Furthermore, in order to repair such damage, it is appropriate to apply the high-early-strength concrete method, since this method can achieve a high level of strength early, has a long storage period for the materials, and has a shorter time for repair [3].

Author Contributions: Conceptualization, I.H.; methodology, I.H.; software, I.H.; validation, I.H., J.H. and S.K.; formal analysis, I.H.; investigation, S.K.; resources, I.H.; data curation, I.H.; writing—original draft preparation, I.H.; writing—review and editing, I.H. and J.H.; visualization, S.K.; supervision, I.H.; project administration, I.H.; funding acquisition, J.H. All authors have read and agreed to the published version of the manuscript.

Funding: This research received no external funding.

Acknowledgments: This study has been performed with support from Seoul National University of Science and Technology in Korea.

Conflicts of Interest: The authors declare no conflict of interest.

References

1. Kenneth, C.; Ove, D.; Jenzen-Jones, N.R.; Marc, G. *Explosive Weapons in Populated Areas: Technical Considerations Relevant to Their Use and Effects*; Armament Research Services (ARES): Canberra, Australia, 2016. Available online: https://reliefweb.int/sites/reliefweb.int/files/resources/aresweb-generic.pdf (accessed on 22 December 2021).
2. Wu, J.; Chew, S.H. Field performance and numerical modeling of multi-layer pavement system subject to blast load. *Sci. Constr. Mater.* **2014**, *52*, 177–188. [CrossRef]
3. Mo, L.; Victor, C. High-Early-Strength Engineered Cementitious Composites for Fast, Durable Concrete Repair—Material Properties. *ACI Mater. J.* **2011**, *108*, 3–12.
4. Air Force Tactics, Techniques, and Procedures. *Airfield Damage Assessment after Major Attack. Air Force Tactics, Techniques, and Procedures*; ATTP 3-32.11; Department of the Air Force: Virginia Beach, VA, USA, 2016.
5. Kim, S.H.; Tomas, H.; Kang, K. Development of Energy-Based Impact Formula-Part I: Penetration Depth. *Appl. Sci.* **2020**, *10*, 4964. [CrossRef]
6. UFC. *Design and Analysis of Hardened Structures to Conventional Weapons Effects*; UFC 3-340-01; USA Department of Defense: Washington, DC, USA, 2002.
7. Rama, C.M.A.; Palani, G.S.; Nagesh, R.I. Evaluation of Concrete Penetration Depth under Impact Loading Employing Empirical Formula. *SDHM* **2008**, *4*, 221–229.
8. Frew, D.J.; Hanchak, S.J.; Green, M.L.; Forrestals, M.J. Penetration of concrete targets with ogive nose steel rods. *Int. J. Impact Eng.* **1998**, *21*, 489–497. [CrossRef]
9. Bulson, P.S. *Explosive Loading of Engineering Structures*; Taylor & Francis e-Library: London, UK, 1997.
10. Kingery, C.N.; Bulmash, G. *Technical Report ARBRL-TR-02555: Air Blast Parameters from TNT Spherical Air Burst and Hemispherical Burst*; AD-B082 713; U.S. Army Ballistic Research Laboratory, Aberdeen Proving Ground: Adelphi, MD, USA, 1984.
11. Hwang, I.J.; Kim, S.K. Field Performance and Rapid Repair Method of an Airfield Pavement under the Blast Load of Cluster Bomb Unit, WMCAUS 2021. *IOP Conf. Ser. Mater. Sci. Eng.* **2021**, *1203*, 032070. [CrossRef]
12. Advisory Circular of US. *Pavement Design and Evaluation*; AFPAM, AC 150/5320-6F; Advisory Circular of U.S. Department of Transportation Federal Aviation: Washington, DC, USA, 2016.
13. Karlos, V.; Solomos, G. *Calculation of Blast Loads for Application to Structural Components*; JRC Technical Reports; Publications Office of the European Union: Luxembourg, 2013; p. 8.
14. US. Department of Energy, Amarillo Energy Office. *A Manual for the Predictions of Blast and Fragment Loadings on Structures*; DOE/TIC-11268; US. Department of Energy, Amarillo Energy Office: Amarillo, TX, USA, 1981; pp. 79–101.
15. Brode, H.L. Numerical solution of spherical blast waves. *J. Appl. Phys.* **1955**, *26*, 766–775. [CrossRef]
16. Mills, C.A. The design of concrete structures to resist explosions and weapon effects. In Proceedings of the 1st International Conference on Concrete for Hazard Protections, Edinburgh, UK, 27–30 September 1987.

17. Malvar, L.J.; Crawford, J.E.; Wesevich, J.W.; Simons, D. A plasticity concrete material model for DYNA3D. *Int. J. Impact Eng.* **1997**, *19*, 847–873. [CrossRef]
18. Alia, A.; Souli, M. High explosive simulation using multi-material formulations. *Appl. Therm. Eng.* **2006**, *26*, 1032–1042. [CrossRef]
19. Christian, H.; Jürgen, S. Comparison of the RHT Concrete Material Model in LS-DYNA and ANSYS AUTODYN. In Proceedings of the 11th European LS-DYNA Conference 2017, Salzburg, Austria, 9–11 May 2017.
20. Park, D. Numerical Models for Simulating the Dynamic Behavior of Concrete Subjected to High Velocity Impact. *J. Korean Soc. Miner. Energy Resour. Eng.* **2017**, *54*, 429–436. [CrossRef]
21. Herrmann, W. Constitutive Equation for the Dynamic Compaction of Ductile Porous Materials. *J. Appl. Phys.* **1969**, *40*, 2490–2499. [CrossRef]
22. Holmquist, T.J.; Johnson, G.R.; Gooch, W.A. Modeling the 14.5 mm BS41 projectile for ballistic impact computations. *WIT Trans. Model. Simul.* **2005**, *40*, 61–75.
23. Thomas, B.; Riedel, W. The Rht Concrete Model in Ls-Dyna. In Proceedings of the 8th European LS-DYNA Users Conference, Strasbourg, France, 24 May 2011.
24. Ryu, Y.-S.; Cho, H.-M.; Kim, S.-H. Collision Behavior Evaluatio of Flexible Concrete Mattress Depending on Material Models. *J. Ocean. Eng. Technol.* **2015**, *29*, 70–77. [CrossRef]
25. Riedel, W.; Kawai, N.; Kondo, K.-I. Numerical assessment for impact strength measurements in concrete materials. *Int. J. Impact Eng.* **2009**, *36*, 283–293. [CrossRef]
26. Robert, H. *IHS Jane's Weapons: Air Launched 2014–2015*; FSC: Llanidloes, UK, 2014.